PYROLYSIS STUDY OF A HYDRIDE–SOL–GEL SILICA
Part I. Chemical aspects

R. Campostrini[*], *A. Sicurelli, M. Ischia and G. Carturan*

Dipartimento di Ingegneria dei Materiali e Tecnologie Industriali, Universitť di Trento, via Mesiano 77, 38050 Trento, Italy

A homogeneous silica gel sample bearing ≡Si–H groups was prepared, via sol–gel method, by hydrolysis of trimethoxysilane under acid condition in tetrahydrofuran. Preliminary NMR experiments in liquid phase indicated an immediate and complete hydrolysis of Si–OCH$_3$, followed by a slower condensation of the Si–OH groups, with maintenance of Si–H bonds. The crude-gel, and samples heated to various temperatures, were characterized by different instrumental methods, including FTIR, density, porosity, and specific surface area. These data indicate that the crude-gel was a dense material which, on heating, increases porosity and surface area up to ca. 500°C.

The thermal behavior was studied in inert atmosphere by means of coupled thermogravimetric, gas chromatographic, mass spectrometric analyses. The pyrolysis process was described by the fundamental chemical reactions occurring among the siloxane chains of the gel network and by the qualitative and semiquantitative chemical analysis of the compounds released in gas-phase. The proposed pyrolysis mechanism was discussed and interpreted in agreement with the change of the morphological properties of the gel. The pyrolysis data and the mass balance between the compounds released in gas-phase and the solid residue at 1000°C allowed the determination of a nominal chemical formula to describe the crude-gel composition.

Keywords: hydride silica gel, pyrolysis study, sol–gel synthesis, thermogravimetric-mass spectrometric gas chromatographic coupled analyses

Introduction

The use of XSi(OR)$_3$ alkoxides (X=alkyl, H, F) as precursors of SiO$_2$-based xerogels constitutes an ordinary process artifact to obtain ormosil [1–3] and/or ormocer [4] materials and, more in general, advanced materials. The presence of the Si–X functional groups, which are unsuitable for immediate hydrolysis, may lead to formation of Si–O–Si gel networks, substantially maintaining the Si–X bonds which determine a wide variability of features such as porosity, surface area, hardness, and wettability. Moreover, XSiO gels under controlled thermal treatment undergo specific reactions that involve Si–X bond cleavage and that promote deep adjustments of the siloxane network born out by Si–OR hydrolysis and condensation. For example, in the case of X=CH$_3$, new Si–C bonds can be formed, leading to oxycarbide glasses in which the cross-linking due to C bonding modes improves the final solid properties [5–7]. In other cases, silicon units or oligomers can be formed and released in the gas phase by Si–X/Si–O bond exchanges among vicinal siloxane chains: the mass loss leads to a valuable increase of porosity which contrasts the expected densification due to the thermal treatment [8–11].

With the perspective of obtaining metallic dispersions in a silica matrix, HSi(OR)$_3$ alkoxide precursors present a valuable advantage due to the presence of hydride group which may be used for tailored reduction of metallic species introduced in the original gelling solution [12, 13]. As a matter of fact, the modest Si–H reduction power, the metallic ion reduction potential, and the variable ligand coordination may all be activated or adjusted by controlled thermal treatments. This aspect may be not trivial since the homogeneous metal ion dispersion in the gelling solution is maintained in the xerogel. The reduction, therefore, produces single atoms, which present a hindered collapse to high dimension particles owing to the diffusion limitation from the siloxane network [14–16]. Moreover, the above mentioned high temperature mass loss of silicon-X units, can promote the increase of the porosity and of the active surface of the siliceous matrix, ultimately inducing high temperature porosity collapse, which may be detrimental, for instance, in gas-sensor and catalysis performance.

These arguments spurred us to study the chemical behavior of HSi(OCH$_3$)$_3$ for sol-gel processing in tetrahydrofuran solution, and the thermal behavior of prepared xerogels. Indeed, this alkoxide presents a simple molecular structure and exalted reactivity in Si–OCH$_3$ hydrolysis and condensation due to the low steric hindrance of the methoxy group and the polarity of the Si–H bond [17]. These properties led us to consider HSi(OCH$_3$)$_3$ as a pattern XSi(OR)$_3$ alkoxide, and oriented us toward studying the morphological

features of the crude xerogel and its thermal stability. The network rearrangements, which occur in the solid gel during heating up to 1000°C, were studied by coupled thermogravimetric-gas chromatographic and mass-spectrometric measurements.

Experimental

Chemicals

Trimethoxysilane (95%) was purchased from ABCR and used without any further purification. A 0.01 M hydrochloric water solution was prepared by dilution of Carlo Erba pure reagent (HCl 37%, d=1.186 g cm^{-3}). Tetrahydrofuran (THF) (anhydrous, 99.9%, Aldrich) was previously dried by distillation on Na/benzophenone. 2,5-Dihydrofuran (97%, Aldrich) was used as standard for gas chromatographic analysis. Tetrahydrofuran-d_8 (99.5% D), chloroform-d (99.96% D) and deuterium oxide (99.99% D) used in NMR measurements were Aldrich pure products.

Instrumentation

FTIR spectra were recorded on a Nicolet Avatar 330 spectrometer in transmission mode in the 4000–400 cm^{-1} range. Powdered samples were analyzed in KBr pellets by collecting 64 scans with 4 cm^{-1} resolution working in the air.

Specific surface areas and pore size values were determined by N_2 adsorption at 77 K on an ASAP2010 Micromeritics analyzer. Equilibrium points were considered inside the 0.05–0.33 p/p_0 range; data were processed by BET and BJH equations [18, 19].

Density measurements were carried out on a Micromeritics 1305 multivolume He pycnometer; amounts of ca. 100 mg of powdered samples were analyzed.

Thermogravimetric (TG) and differential thermal analyses (DTA) were performed on a LabSys Setaram thermobalance operating in the 20–1000°C range, with a heating rate of 10°C min^{-1}. Thermal analyses were recorded working under 100 cm^3 min^{-1} He (99.99%) flux. Powdered samples (13.0 mg) were analyzed using alumina crucibles and α-Al$_2$O$_3$ as reference.

Gas chromatographic analyses (GC) were carried out on a HRGC Carlo Erba Instruments chromatograph coupled with a quadrupole mass spectrometer used as detector. Chromatographic elutions were performed using He as carrier gas (15 kPa inlet pressure), PoraPlot Q (Chrompack) and SE-54 (Mega) capillary columns (25 m, 0.32 mm). A typical temperature program was: 30°C for 5 min followed by 5°C min^{-1} heating rate up to 200°C then maintained for 15 min. Gas phase sampling (volume of 0.1 cm^3) was performed by means of a GR8 (Bimatic) thermostatted (T=130°) microvalve.

The mass spectra analysis (MS) was carried out using a TRIO 1 VG quadrupole mass spectrometer. Electron mass spectra (70 eV) were continuously recorded with frequency 1 scan s^{-1} in the 3–600 amu range.

The pyrolysis studies were performed with two types of instrumental interfaces. A direct and continuous sampling of the gas phase evolved from the solid was realized with the TG-MS coupling, by using a lab-assembled transfer line. This interface is made of 5 m silica capillary column (0.19 mm) thermostatted at 250°C, which connects the thermobalance with the mass spectrometer. This coupling allows the detection of any gas phase released species throughout the pyrolysis process. TG-MS data are recorded as sequence of mass spectra from which it is possible to extrapolate both the total ion current plot (TIC) and the contribution of any m/z ion current graphs (IC) *vs.* time (i.e. temperature of the pyrolysis process). The second interface is based on TG-GC-MS coupling; it allows identification of species simultaneously released during the same mass loss. In this case, the transfer line was connected to the inlet port of the gas chromatographic microvalve. A chromatographic column was used for the elution of the gas mixture, by using the mass spectrometer as detector. Gas phase samplings were done at temperatures corresponding to the main mass losses, during the TG analysis.

A semiquantitative evaluation of pyrolysis data was performed by processing the ion currents of appropriate m/z signals in the TG-MS analysis. By comparing the pattern signals of the mass spectra of all the detected species, the integrated values of suitable ion currents, which can represent and monitor the evolution of each specific species, were used to quantify the amounts of these compounds released during the whole pyrolysis process. Procedure details are reported elsewhere [20–23].

^{1}H NMR spectra were recorded on a Bruker Avance 400, operating at 400.1316 MHz, acquiring 256 scans with 1 s time delay and 10 μs of 90° pulse width. Samples were analyzed in a 5 mm vacuum-sealed NMR tubes (V=0.6 cm^3). The purity and stability of the silicon alkoxide were assessed in tetrahydrofuran-d_8 solution with TMS as internal reference, at 25°C. The intrinsic reactivity of HSi(OCH$_3$)$_3$ with water was followed starting from –70°C up to room temperature.

Results and discussion

Solution behavior of HSi(OCH$_3$)$_3$

The ^{1}H NMR spectrum of the commercially available silicon alkoxide used in the gel synthesis was registered in tetrahydrofuran-d_8 after ca. 2 mounts of the first opening of the original sealed bottle. Signal pat-

tern indicated the predominant presence of $HSi(OCH_3)_3$:hydride signals at 4.09 ppm; $J_{Si–H}$=296 Hz; $SiOCH_3$ signal at 3.52 ppm [24]. The ratio of the hydrogen integrated signals $SiH/SiOCH_3$ was 0.10. This product is unstable and aging affords higher oligomeric species (hydride–methoxy–polysiloxane) responsible for the signals detected in lower extent at higher frequencies (hydride at 4.19 ppm, $SiOCH_3$ at 3.54 ppm). The intensity of these last signals corresponds to the 10% with respect to the monomer ones. Other ^1H signals of OCH_3 groups were detected in the 3.26–3.29 ppm range attributable to alcoholic or ether species (intensity of 8%).

A GC-MS analysis was carried out using a SE-54 column, sampling $1·10^{-3}$ cm^3 of silicon alkoxide. Chromatographic elution showed the presence of ca. 80% of $HSi(OCH_3)_3$, 3% of $Si(OCH_3)_4$, 8% of $(CH_3O)_2HSiOSiH(OCH_3)_2$, 1% of $(CH_3O)_2HSiOSi(OCH_3)_3$, with minor presence of other oligomers (ca. 20 chromatographic peaks, percent values calculated from peak areas) not totally identified and containing up to 4 Si-atoms. GC-MS data are in good agreement with the NMR ones, since the $Si(OCH_3)_4$ resonance is also present at 3.52 ppm according to the integral signal ratio $SiH/Si(OCH_3)$=0.1. Moreover, the H-hydride/Si ratio of ca. 0.85 is also justified by considering the contribution of all the identified species.

In order to study the reactivity of the silicon alkoxide with water, three different tetrahydrofuran-d_8 silicon alkoxide solutions were prepared at –80°C, adding appropriate volumes of a D_2O 0.01 M HCl solution in order to obtain Si-alkoxide/ THF-d_8/D_2O/HCl molar ratios of $0.27/0.88/1/1.8·10^{-4}$, $0.14/0.88/1/1.8·10^{-4}$, and $0.07/0.88/1/1.8·10^{-4}$, respectively. The solutions, closed in vacuum-sealed tubes, were stored at –80°C (4 days) before being analysed. Spectra were recorded starting from –70 up to 25°C, and also analyzing the solutions after 2 days aging. The ^1H NMR spectra, independently from the Si/THF-d_8/D_2O/HCl/ molar ratio of the solutions, indicated that Si–OCH_3 hydrolysis was complete: the CH_3 signal was found at 3.23 ppm, corresponding to free CH_3OD; the Si–H hydride resonance was observed as a complex multiplet in the 4.2–4.4 ppm interval. The integral of Si–H signal between 4.2 and 4.4 ppm and the one of CH_3OD maintain the same ratio observed in the initial Si-alkoxide precursor mixture. As the temperature was increased to 25°C in 30 min, the Si–H resonances appeared as an envelope of signals in the 4.25–4.45 ppm interval, suggesting an increase of molecular complexity. This type of spectrum was also observed after 24 h at room temperature and it resulted independent of the Si/THF-d_8/D_2O/HCl ratios.

The picture resulting from these data accounts for: (i) a very fast hydrolysis of hydride-methoxy-silane or -siloxane species even at –70°C, as demonstrated by the Si–H vs. CH_3OD atomic hydrogen ratio; (ii) a slow condensation of HSi–$(OH)_n$ at –70°C; (iii) a progressive increase in molecular complexity as the temperature increases to 25°C. These results agree with the kinetics of $Si(OCH_3)_4$ reported by Assink and Kay [25–27]. These authors reported that the n=H_2O/Si molar ratio determines the advancement of the hydrolysis for $Si(OCH_3)_{4-n}(OH)_n$ species, the condensation rate of hydrolysed species being about two orders of magnitude less than hydrolysis. In our case, the use n=3 or higher values justifies the immediate hydrolysis of $HSi(OCH_3)_3$ and other hydride–methoxy–siloxane oligomers at –70°C. With this evidence, the absence of methoxy groups in the Si–O–Si cluster growth and the low steric hindrance of Si–H may favour the cluster-to-cluster aggregation, leading to a dense network structure in the final gel, in agreement with the silicic acid gelling behavior reported in [28, 29].

Synthesis of gel-sample

12.6 cm^3 of trimethoxysilane (94.3 mmol) were diluted with 39.0 cm^3 of distilled tetrahydrofuran (0.608 mol), working under nitrogen flow. The solution was cooled to 0°C and treated with 5.1 cm^3 of a 0.01 M HCl solution (0.283 mol of H_2O and $5.1·10^{-5}$ mol of H_3O^+) added dropwise under N_2. After 30 min stirring, the reacting mixture was poured into a vessel and aged in the air at room temperature. The liquid gelled after 5 days, yielding a transparent colourless granular solid.

This gel was milled to a fine powder and dried at room temperature for 2 days, then at 80°C for 5 h. 5.05 g of xerogel were recovered and labelled as HSiO–crude-gel.

Gel features

FTIR spectrum of the crude-gel, Fig. 1, shows a modest broad band centred at 3434 cm^{-1} due to hydrogen-bonded –O–H stretching and an intense sharp peak at 2252 cm^{-1} for the Si–H ones [7, 30]. The very strong asymmetric peak at 829 cm^{-1} results from the ≡Si–H bending, with a shoulder at ca. 875 cm^{-1} attributed to the ≡Si–OH counterpart. The siloxane network gives rise to strong stretching at 1145 (longitudinal optic component) and 1066 cm^{-1} (transverse optic component) in addition to less intense absorptions at 462 cm^{-1} (rocking of the O atoms in the Si–O–Si plane) [31, 32].

The sample heated up to 500°C shows an intense decrease of the ≡Si–H signal and a substantial modification of the siloxane pattern, the shifting of Si–O signals to higher frequencies are in agreement with an increased cross-linking network. As revealed by bend-
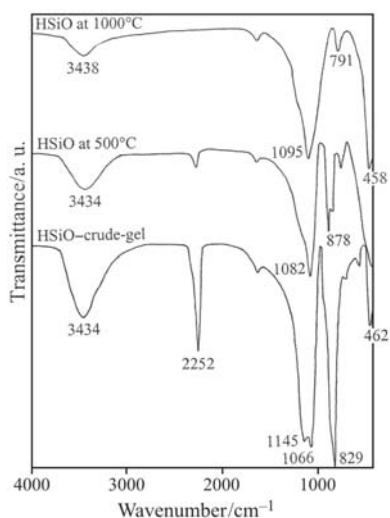
Fig. 1 FTIR spectra of the HSiO–crude-gel and of the samples pyrolyzed up to 500 and 1000°C

ing absorption at 878 cm^{-1}, the $\equiv$Si–OH signal is present, but remarkably decreased. Prolonged heat treatment at 500°C (1 h) yields an almost complete disappearance of the $\equiv$Si–H signal, whereas $\equiv$Si–OH absorptions are still present.

After heat treatment up to 1000°C, the sample shows a more connected siloxane network revealed by the strong asymmetric band at 1095 cm^{-1} (shoulder at ca. 1200 cm^{-1}), followed by two less intense peaks at 791 and 458 cm^{-1}. In this spectra, modest –O–H absorptions are still present. These signals can be attributed to the presence of water molecules only physically adsorbed on the pellet sample, which was handled in the air. (This signal contribution can be assessed as a constant presence in all the samples.)

HSiO–crude-gel presents a specific surface area (*SSA*) of 72($\pm$2) m^2 g^{-1} (BET equation), with average pore diameter (*PD*) =3.0$\pm$0.1 nm and pore volume (*PV*)=0.0279$\pm$2·10^{-4} cm^3 g^{-1} (BJH equation). Pycnometer measurements show density value *d*=1.59$\pm$0.02 g cm^{-3}. The thermal treatment up to 500°C bears an increase of surface area to 360$\pm$2 m^2 g^{-1} with *PD*=3.5$\pm$0.1 nm, and *PV*=0.2645$\pm$2·10^{-4} cm^3 g^{-1}. Further thermal treatments lead to a progressive decrease of both surface area and porosity, in agreement with the expected thermal densification. The sample heated up to 1000°C still shows *SSA*=190$\pm$3 m^2 g^{-1}, *PD*=3.1$\pm$0.1 nm, and *PV*=0.1059$\pm$2·10^{-4} cm^3 g^{-1}.

The results indicate that the crude HSiO xerogel (i.e., the sample aged at 80°C for 5 h) is a dense material still holding an important fraction of $\equiv$Si–H bonds; the thermal treatments over the 500°C yield a drastic consumption of these $\equiv$Si–H moieties, with a valuable increase in porosity and surface area, which are then only smoothly reduced by further heating up to 1000°C.

Pyrolysis process, qualitative description

As shown in Fig. 2, TG curve, recorded at 10°C min^{-1}, shows a continuous mass loss in the range 110–765°C with a total intensity of 7.6%. This loss can be subdivided in three events, according to DTG curve: a first step with a progressive slope in the 110–315°C (1.6%); a more intense central event in the 315–495°C (4.8%); and a latter step in the 495–765°C (1.2%). The DTA curve (not reported) appears to be meaningless, showing a coarse broad endothermic band during the whole mass loss range.
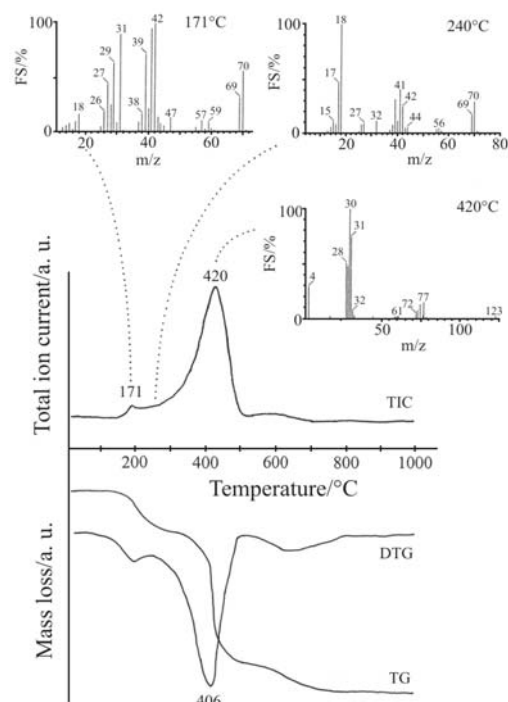
Fig. 2 Thermogravimetric mass spectrometric coupled analysis of HSiO–crude-gel. TG and DTG curves with the total ion current (TIC) plot of the evolved gas phase *vs.* pyrolysis temperature. In the insets, mass spectra recorded at definite temperatures

The evolved gas phase leads to a total ion current curve (TIC) characterized by an initial small peak centred at 171°C, followed by an intense asymmetric (fronting) band at 420°C. The trend of this curve is very similar to the DTG one, confirming the efficiency of the instrumental TG-MS interface. Recorded mass spectra corresponding to the highest TIC peak (inset of Fig. 2, 420°C) show a pattern of intense signals (*m/z* 28–33) attributed to SiH$_4$, and other two sets of fragmentation ions (*m/z* 58–61 and 72–78) assigned to H$_3$SiOCH$_3$ and H$_3$SiOSiH$_3$, respectively. In these spectra, the *m/z* 123 signal is also detected. Mass spectra, recorded in the early fronting part of this TIC peak (inset 240°C), show the main presence of H$_2$O (*m/z* 16, 17, 18) with a group of signals which

becomes the most important pattern in the spectra recorded for the small peak at 171°C (inset 171°C, m/z 15, 39, 41, 42, 69, 70). These signals are due to an organic species release.

In order to obtain better identification of released compounds, some TG-GC-MS analyses were also carried out using appropriate amounts of initial HSiO–crude-gel. In Fig. 3, the gas chromatographic elutions of the gas phase, sampled at 171 and 420°C, are reported. At 171°C, 2,5-dihydrofuran and water, to a lesser extent, are observed; silane and minor amounts of disiloxane and methoxysilane were found in the 420°C sampling. The presence of dihydrofuran was unexpected, tetrahydrofuran being the solvent used in the synthesis; the release of silane-derivate compounds were expected, by considering the precursor nature and the reactivity of the $\equiv$Si–H group.

Taking into account the mass spectra of detected compounds (and their estimated relative amounts), appropriate m/z ions where selected to follow the evolution of these species throughout the pyrolysis process. The ion currents of these representative ions are reported in Fig. 4. The release of water (m/z 18) is distributed in a wide temperature range, by a broad band centred at 237°C, and in a second modest one at 468°C. Dihydrofuran (m/z 70) is the first species released, showing two overlapped peaks at 171 and 210°C. Silane (m/z 31), methoxysilane (m/z 61), and disiloxane (m/z 77) are closely released, as shown by

bands centred at 424, 405 and 403°C, respectively; their trends yield the shape of the main peak of the TIC curve. The m/z 123 signal, detected in the mass spectra recorded inside this TIC peak, is attributed to the deprotonated fragment ion of trisiloxane: $H_3SiOSi(H)_2OSiH_3$. The trend of the m/z 123 ion current is quite similar to the other silane species, having a maximum release at 398°C.

According to previously pyrolysis studies on silica gels functionalised by $\equiv$Si–H, $\equiv$Si–CH$_3$ and $\equiv$Si–F groups, the thermal behavior of this HSiO–crude-gel has been explained by considering three different chemical events: first, the release of solvent molecules physically entrapped in the siloxane network; the thermal condensation of vicinal silanol groups surviving the gelling process; and the release of silane monomers and even of siloxane oligomers, by exchange reactions between Si–H and Si–O bonds among the siloxane chains.

The aging and drying processes usually allow complete removal of entrapped solvent molecules (alcohol) in gels obtained from silicon alkoxide precursor; in fact, the release of ethanol in gas phase was rarely observed in our gels. The high reactivity of hydride–methoxy–silane precursor mixture towards hydrolysis, the rapid growth of the siloxane chains inside the liquid phase, and the high solvent amount used in this preparation all favor the formation of a gel structure with low porosity and low specific sur-
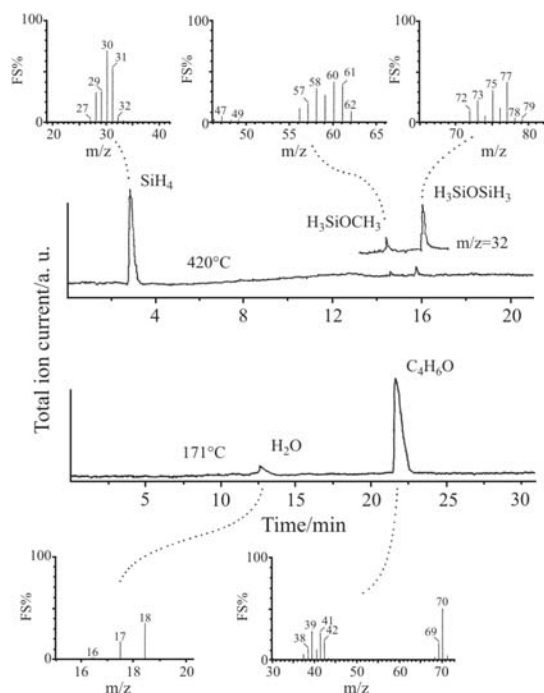
Fig. 3 Gas chromatographic elutions of the gas phase released at 171 and 420°C during the pyrolysis of the HSiO–crude-gel
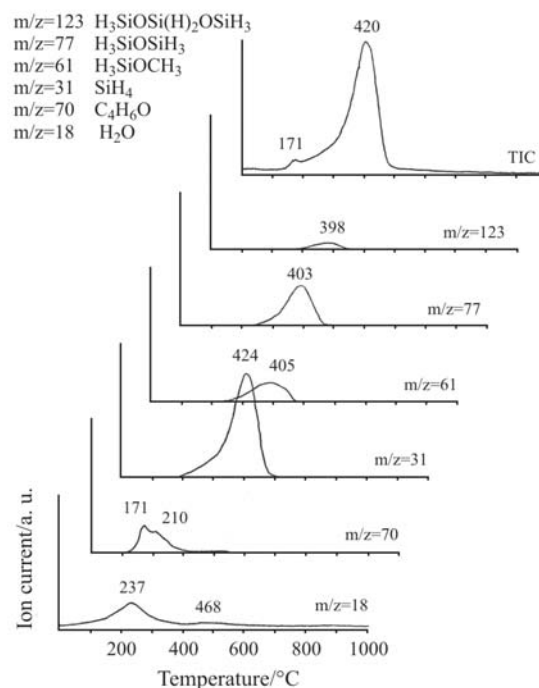
Fig. 4 Thermogravimetric mass spectrometric coupled analysis of HSiO–crude-gel. Ion currents of selected ions used to monitor specific evolved species during pyrolysis process

face area. These facts may also justify the unusual tetrahydrofuran solvent entrapping. In fact, dihydrofuran was the species detected, as confirmed by a GC-MS measure carried out on a pure sample. A particular chemical interaction by the hydride-silica matrix and the entrapped tetrahydrofuran must be invoked to account for the dehydrogenation to dihydrofuran, whose release also implies a stoichiometric H_2 formation (not detectable by our apparatus). Finally, the temperature interval of the dihydrofuran detection is still compatible with the simple release of molecules physically entrapped in a gel-network.

As for the second event, according to IR analysis, HSiO–crude-gel shows a valuable presence of hydroxyl groups. Although a fraction of released water may arise from physically entrapped molecules at the early stage of heating, the condensation of vicinal silanol groups progressively yields water evolution with a cross-linking of the siloxane chains, Reaction 1.

This process is spread across a wide temperature range as shown by the bimodal trend of the m/z 18 ion current. This thermally activated condensation is re-

sponsible for the progressive collapse of the gel network to a less porous structure, as revealed by the porosity reduction of samples heated to temperatures above the main mass loss (i.e., $T > 500°C$).

Above 300°C, the breaking of the $\equiv$Si–H and $\equiv$Si–O bonds allows a deep rearrangement of the siloxane network. By $\equiv$Si–H/$\equiv$Si–O bond exchanges, some silicon atoms along the siloxane chains can be enriched with hydrogen, yielding species no longer linked to the Si–O–Si polymer network. Therefore, three-bond exchanges on a $\equiv$Si–H silicon atom of the gel afford volatile SiH_4, Reaction 2. Two-bond exchanges on the small amount of silicon atoms still bearing an uncondensed methoxy group lead to H_3SiOCH_3 release, Reaction 3.

Moreover, even small fragments of the siloxane chains (containing few Si atoms) can be released by the same bond exchanges, involving different vicinal Si atoms, as described in Reaction 4 for the disiloxane species.
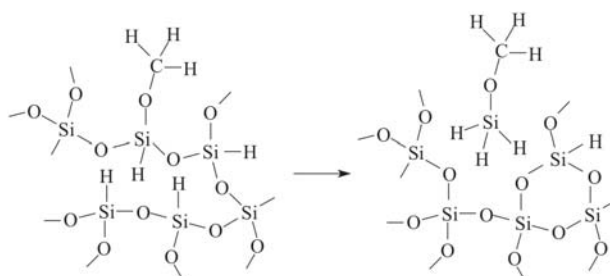
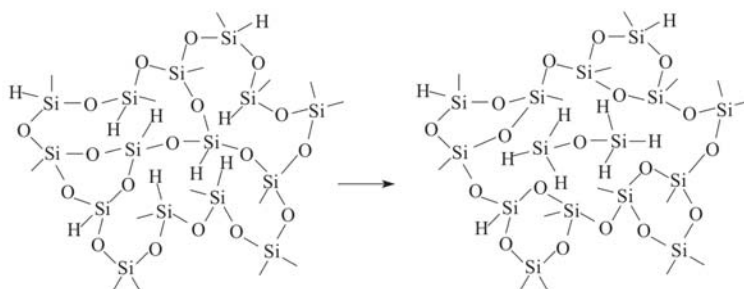The driving force of these siloxane chain rearrangements may be attributed to the favourable
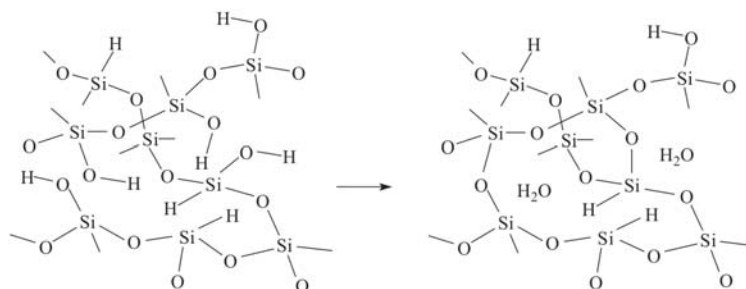
Reaction 1 Water released by silanol group condensation
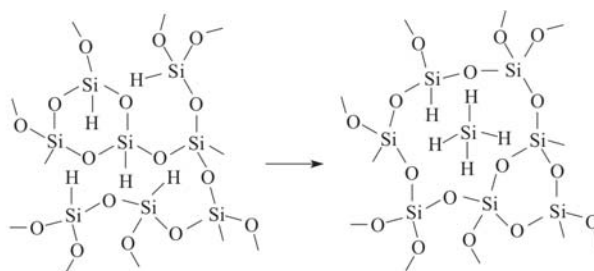
Reaction 2 Silane release by Si–H/Si–O bond exchange

Reaction 3 Methoxysilane release by Si–H/Si–O bond exchange

Reaction 4 Disiloxane release by Si–H/Si–O bond exchange

entropic change due to gas phase release, enthalpy contribution being quite low owing to maintenance of the same number of Si–H and Si–O bonds. The gas phase release of silane (or small siloxanes) is responsible for rapid mass loss around 410°C. The concomitant formation of holes inside the SiO_2 network accounts for a sudden, valuable porosity increase, resulting in a narrow dispersion of pore dimensions. All these reactions lead to consumption of $\equiv$Si–H bonds inside the gel structure according to IR data of samples heated up to 500°C. Consequently, the drastic decrease of the $\equiv$Si–H group density in the gel rapidly quench its mass loss.

Above 500°C, the main species released is water again, as detected by TG-MS analysis. The low density of the remaining silanol groups accounts for the reduced intensity of the gel mass loss in the 495–765°C range, as well as for the modest shrinkage of the gel network. Actually, porosity and surface area of the sample heated up to 1000°C are quite high. Surprisingly, these values are even higher than those of the initial gel.

Pyrolysis process, semi-quantitative description

The thermogravimetric-mass spectrometric analysis (at 10°C min^{-1}) was carried out on 13.0 mg of HSiO–crude-gel, which presented at 1000°C a total mass loss of 7.6%, yielding 12.01 mg of residual solid

and 0.99 mg of evolved gas phase. The main species released for the entire pyrolysis was SiH_4 with minor amounts of H_2O, dihydrofuran, H_3SiOCH_3, $H_3SiOSiH_3$, and traces of $H_3SiOSi(H)_2OSiH_3$. Each species ('j') can be monitored by a suitable m/z ion (labelled as representative ion 'i^*') among those detected in their mass spectra recorded in the TG-GC-MS analyses. In the case of $H_3SiOSi(H)_2OSiH_3$, its lack detection in TG-GC-MS measurements (due to the extremely low amount) makes it necessary to assume that its mass spectrum is constituted only by the m/z 123 signal. Table 1 summarizes the fragment ions, and their relative intensities ('$r(i)_j$') that were detected in the mass spectra of these compounds. For each representative ion, the area value of its ion currents, calculated for the whole pyrolysis process, is also reported ('$Im/z(i^*)_j$'). From these data, the integrated amount, which quantifies the relative amount revealed by the mass spectrometer detector for each compound, is calculated ('$A(j)=Im/z(i^*)_j/r(i)_j$'). By considering the integrated amounts of all the detected species, the molar (and mass) percentage composition of the gas phase evolved during the entire pyrolysis is first deduced. These data are then converted in effective moles of released compounds, taking into account the total 0.99 mg of evolved gas, as reported in Table 2.

Data processing indicates that SiH_4 is the most important compound released (78.3%$_{mol}$) followed by the disiloxane species (12.1%$_{mol}$), whose release is statistically less probable as it requires four

Table 1 Data from mass spectra of the chemical species detected in TG-MS and TG-GC-MS measurements and from the integrated values of m/z ion currents

Chemical species 'j', representative ion '$m/z(i^*)_j$' [integrated m/z value obtained by TG-MS analysis '$Im/z(i^*)_{TG-MS}$'/a. u.]	Main m/z fragment ions in mass spectra of substances recorded in TG-GC-MS analyses '$m/z(i)_j$' (peak height/a. u.)	Relative intensity of representative ion '$r(i^*)_j$'	Integrated amount '$A(j)$'/a.u.
H_2O, 18 [$2.087 \cdot 10^7$]	8 (18); 17 (9); 16 (2)	0.6207	$3.363 \cdot 10^7$
Dihydrofuran, 70 [$4.419 \cdot 10^6$]	70 (5); 69 (3); 42 (8); 41 (9); 39 (6)	0.1613	$2.740 \cdot 10^7$
SiH_4, 31 [$1.844 \cdot 10^8$]	32 (5); 31 (64); 30 (88); 29 (41); 28 (39)	0.2700	$6.827 \cdot 10^8$
H_3SiOCH_3, 61 [$7.343 \cdot 10^6$]	61 (3); 60 (2); 59 (1.5); 58 (1.5);	0.3750	$1.958 \cdot 10^7$
$H_3SiOSiH_3$, 77 [$4.263 \cdot 10^7$]	78 (1.5); 77 (18); 75 (13); 73 (8); 72 (4)	0.4045	$1.054 \cdot 10^8$
$H_3SiOSi(H)_2OSiH_3$, 123 [$3.334 \cdot 10^6$]	123 (5)	1	$3.334 \cdot 10^6$

Integrated value of TIC curve=$9.378 \cdot 10^8$

Table 2 Chemical composition of the gas mixture evolved in the whole pyrolysis process of HSiO–crude-gel sample

Chemical species 'j' (molecular mass)	Mol/%	Mass/%	Moles
H_2O (18.02)	3.85	1.77	$9.68 \cdot 10^{-7}$
Dihydrofuran (70.09)	3.14	5.60	$7.89 \cdot 10^{-7}$
SiH_4 (32.12)	78.30	63.85	$1.97 \cdot 10^{-5}$
H_3SiOCH_3 (62.14)	2.24	3.55	$5.64 \cdot 10^{-7}$
$H_3SiOSiH_3$ (78.22)	12.08	24.02	$3.03 \cdot 10^{-6}$
$H_3SiOSi(H)_2OSiH_3$ (124.32)	0.38	1.21	$9.60 \cdot 10^{-8}$

$\equiv$Si–H/$\equiv$Si–O bond exchanges instead the three necessary for silane. Although methoxysilane evolution requires only two-bond exchanges, the low number of silicon atoms still bearing a methoxy group after gelling justifies the low presence (2.2%$_{mol}$) of H_3SiOCH_3. In the 100–750°C range, water release (3.8%$_{mol}$) is observed in two events, i.e., before and after the gel network rearrangement (315–495°C). Before the siloxane chain rearrangements, the stripping of the solvent from the crude-gel evolves dihydrofuran (3.1%$_{mol}$). The proposed pyrolysis mechanism, in terms of reactions and amounts of released species, accounts for the 93% of the total amount of signal recorded by the mass spectrometer detector during the entire TG-MS analysis (i.e., of the integrated value of the TIC curve).

As shown by IR spectrum, the 12.01 mg of solid recovered after pyrolysis at 1000°C can be considered a pure SiO_2 matrix containing $2.0 \cdot 10^{-4}$ mol of Si atoms and $4.0 \cdot 10^{-4}$ of bridging O atoms. Considering the amounts of all the silane derived species and the water detected in gas phase (Table 2), $2.66 \cdot 10^{-5}$ mol of Si atoms, $4.76 \cdot 10^{-6}$ mol of O, $5.64 \cdot 10^{-7}$ mol of C, and $1.03 \cdot 10^{-4}$ mol of H are calculated in the evolved compounds, taking into account the stoichiometric equations reported in Scheme 1 that are deduced from Reactions 1–4. A further $7.89 \cdot 10^{-7}$ mol of dihydrofuran plus a stoichiometric amount of molecular hydrogen are counted for the stripped solvent mole-
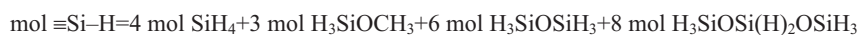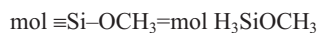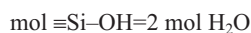
cules. From these data, a nominal amount of 12.99 mg is calculated for the mass of the starting gel sample. This mass balance checks both the validity of the proposed pyrolysis mechanism, and the qualitative- and quantitative-gas phase analyses. The same calculations allow determination of the moles of functional groups present in the HSiO–crude-gel, and the proposal of a nominal formula to describe its chemical composition: $H_{0.438}SiO_{1.775}(OH)_{0.008}(OCH_3)_{0.002}$. This accounts for the high degree of crosslinking of the gel structure (due to the substantial amount of bridging oxygen atoms), and agrees with the high density value found for the crude-gel when compared with samples prepared in similar conditions starting from other silicon alkoxides. The high hydrolysis rate of $HSi(OCH_3)_3$ yields a gel structure with a low presence of unhydrolyzed methoxy groups (ca. 0.2%). Nevertheless, the intrinsic high reactivity of HSi–(OH) species favors the extensive condensation of silanol groups (uncondensed $\equiv$Si–OH/Si-atoms <1%). The unexpected low presence of $\equiv$Si–H groups (ca. 44%) deserves some specific comments.

The ^{1}H NMR results indicate that hydrolysis of HSi–OCH$_3$ species is virtually completed before condensation, which consequently involves only the HSi–OH counterpart. Since we used acid catalysis conditions, the transition state of the condensation reaction involves the nucleophilic attack of HSi–OH on the central Si of another activated $HSi–OH_2^+$ species. As this intermediate is formed, the leaving group effect may discriminate between condensation processes, with release of H_2O or of H_2. For the latter, a higher temperature may be required, and may preferentially occur on the solid gel during aging at 80°C or during the early stage of the heating. Since the steric hindrance of the hydride is very low, the preferential occurrence of linear oligomers under acid catalysis is not expected [33, 34]. Accordingly, the condensation between $\equiv$Si–OH's or between $\equiv$Si–OH and $\equiv$Si–H can effectively bear dense Si–O–Si clusters, as ascertained by the high density and low porosity of the crude-gel.

Scheme 1 Stoichiometric equations for evaluating the moles of elements contained in the compounds detected in the gas phase and evolved during the whole pyrolysis process

mol Si=mol SiH_4+mol H_3SiOCH_3+2 mol $H_3SiOSiH_3$+3 mol $H_3SiOSi(H)_2OSiH_3$

mol O=mol H_2O+mol H_3SiOCH_3+mol $H_3SiOSiH_3$+2 mol $H_3SiOSi(H)_2OSiH_3$

mol C=mol H_3SiOCH_3

mol H=2 mol H_2O+4 mol SiH_4+6 mol H_3SiOCH_3+6 mol $H_3SiOSiH_3$+8 mol $H_3SiOSi(H)_2OSiH_3$

Stoichiometric equations for evaluating the moles of functional groups present in the starting gel sample

mol $\equiv$Si–OH=2 mol H_2O

mol $\equiv$Si–OCH$_3$=mol H_3SiOCH_3

mol $\equiv$Si–H=4 mol SiH_4+3 mol H_3SiOCH_3+6 mol $H_3SiOSiH_3$+8 mol $H_3SiOSi(H)_2OSiH_3$

Conclusions

The gelling of 'HSi(OCH₃) mixtures' in tetrahydrofuran under acid catalysis with a $H_2O/Si=3$ molar ratio at 80°C afforded a solid gel preserving 44% of original Si–H bond. The peculiar reactivity of the hydride–methoxy–silane mixture leads to a gel characterized by low porosity and high density.

The pyrolysis study, carried out by coupling TG-MS and TG-GC-MS analyses, allowed: identification of the gaseous products released from the gel during heating; formulation of single reaction mechanisms for each released species. Gel pyrolysis process was described by three subsequent events, partially overlapped. (A), the stripping of the solvent molecule physically entrapped in the gel network; this process was also accompanied by the dehydrogenation of the released tetrahydrofuran. (B), the release of water, in a bimodal trend, by condensation of residual ≡Si–OH groups. This thermal condensation was responsible for the modest, but progressive, densification that the gel matrix underwent before and after its main mass loss around 410°C. (C), the evolution of silanes and small siloxane species, by ≡Si–H/≡Si–O bond exchanges along the siloxane chains of the gel network. These network rearrangements yielded to rapid consumption of the ≡Si–H groups in the gel structure, leading to an increase in its porosity.

Finally, the semi-quantitative TG-MS data processing allowed quantification of the released compounds and the functional groups present in the crude-gel, leading to a stoichiometric formula that describes its initial chemical composition.

Acknowledgements

References

1 P. Judeinstein and C. Sanchez, J. Mater. Chem., 6 (1996) 511.

2 D. A. Loy, Mat. Res. Soc. Bull., 26 (2001) 364.

3 C. Sanchez and B. Lebeau, Mat. Res. Soc. Bull., 26 (2001) 377.

4 R. Nass, E. Arpac, W. Glaubitt and H. Schmidt, J. Non-Cryst. Solids, 121 (1990) 370.

5 G. D. Sorarů, G. D'Andrea, R. Campostrini, F. Babonneau and G. Mariotto, J. Am. Ceram. Soc., 78 (1995) 379.

6 G. D. Sorarů, G. D'Andrea, R. Campostrini and F. Babonneau, in Sol-Gel Science and Technology, Eds E. J. A. Pope, S. Sakka and L. C. Klein, Ceramic Transactions 55, Publ. Am. Cer. Soc., Westerville, Ohio 1995, pp. 135–146.

7 G. D. Sorarů, G. D'Andrea, R. Campostrini and F. Babonneau, J. Mater. Chem., 5 (1995) 1363.

8 R. Campostrini, G. D'Andrea, G. Carturan, R. Ceccato, and G. D. Sorarů, J. Mater. Chem., 6 (1996) 585.

9 G. D. Sorarů, R. Campostrini, G. D'Andrea and S. Maurina, Mat. Res. Soc. Symp. Proc., 435 (1996) 381.

10 R. Campostrini, M. Ischia, G. Carturan and L. Armelao, J. Sol-Gel Sci. Technol., 23 (2002) 107.

11 R. Campostrini, M. Ischia and L. Armelao, J. Therm. Anal. Cal., 78 (2004) 675.

12 R. Campostrini and S. Dirč, Proceeding of Eurogel 92, Colmar 1995, pp. 307–212.

13 S. Dirč, R. Ceccato, G. Facchin and G. Carturan, J. Mater. Chem., 11 (2001) 678.

14 R. Campostrini, G. Carturan, S. Dirč and P. Scardi, J. Mol. Catal., 53 (1989) L13.

15 R. Campostrini, G. Carturan and R. M. Baraka, J. Mol. Catal., 78 (1993) 169.

16 R. Campostrini, M. Ischia, G. Carturan, S. Gialanella and L. Armelao, J. Sol-Gel Sci. Techn., 18 (2000) 61.

17 J. Livage and M. Henry in 'Ultrastructure Processing of Advanced Ceramics', Eds J. D. Mackenzie and D. R. Ulrich, Wiley, New York 1988, pp. 183–195.

18 S. J. Gregg and K. S. W. Sing, Adsorption, Surface Area and Porosity, Academic Press, London 1982.

19 P. A. Webb and C. Orr, Analytical Methods in Fine Particles Technology, Ed. Micromeritics Instrument Corporation, Norcross, USA 1997.

20 R. Campostrini, M. Ischia and L. Palmisano, J. Therm. Anal. Cal., 71 (2003) 997.

21 R. Campostrini, M. Ischia and L. Palmisano, J. Therm. Anal. Cal., 71 (2003) 1011.

22 R. Campostrini, M. Ischia and L. Palmisano, J. Therm. Anal. Cal., 75 (2004) 13.

23 R. Campostrini, M. Ischia and L. Palmisano, J. Therm. Anal. Cal., 75 (2004) 25.

24 B. J. Aylett, Inorg. Chem. Radiochem., 11 (1968) 249.

25 R. A. Assink and B. D. Kay, J. Sol-Gel Sci. Technol., 99 (1988) 359.

26 R. A. Assink and B. D. Kay, J. Sol-Gel Sci. Technol., 104 (1988) 112.

27 R. A. Assink and B. D. Kay, J. Sol-Gel Sci. Technol., 107 (1988) 35.

28 S. H. Garofalini and G. E. Martin, J. Phys. Chem., 98 (1994) 1311.

29 K. Yamahara and K. Okazaki, Fluid Phase Equilib., 144 (1998) 449.

30 N. B. Colthup, L. H. Daly and S. E. Wiberley, Introduction to Infrared Raman Spectroscopy, Ed. Academic Press, San Diego, CA 1990.

31 M. C. Matos, L. M. Ilharco and R. M. Almeida, J. Non-Cryst. Solids, 147, 148 (1992) 232.

32 P. Innocenzi, J. Non-Cryst. Solids, 2316 (2003) 309.

33 R. K. Iler, The Chemistry of Silica, Wiley, New York 1979.

34 C. J. Brincker and G. W. Scherer, Sol-Gel Science: The Physics and Chemistry of Sol-Gel Processing, Ed. Academic Press, San Diego CA 1990.